

# Strong Correlation Effects of A-site Ordered Perovskite $\text{CaCu}_3\text{Ti}_4\text{O}_{12}$ revealed by Angle-Resolved Photoemission Spectroscopy

H. J. Im,<sup>1,\*</sup> M. Tsunekawa,<sup>2</sup> T. Sakurada,<sup>1</sup> M. Iwataki,<sup>1</sup> K. Kawata,<sup>1</sup> T. Watanabe,<sup>1</sup> K. Takegahara,<sup>1</sup> H. Miyazaki,<sup>3</sup> M. Matsunami,<sup>4,5</sup> T. Hajiri,<sup>4,6</sup> and S. Kimura<sup>4,5</sup>

<sup>1</sup>*Department of Advanced Physics, Hirosaki University, Hirosaki 036-8224, Japan*

<sup>2</sup>*Faculty of Education, Shiga University, Shiga 522-8522, Japan*

<sup>3</sup>*Department of Environmental and Materials Engineering,  
Nagoya Institute of Technology, Nagoya 466-8555, Japan*

<sup>4</sup>*UVSOR Facility, Institute for Molecular Science, Okazaki 444-8585, Japan.*

<sup>5</sup>*School of Physical Sciences, The Graduate University  
for Advanced Studies, Okazaki 444-8585, Japan.*

<sup>6</sup>*Graduate School of Engineering, Nagoya University, Nagoya 464-8603, Japan*

(Dated: March 20, 2013)

## Abstract

We report angle-resolved photoemission spectroscopy (ARPES) results of A-site ordered perovskite  $\text{CaCu}_3\text{Ti}_4\text{O}_{12}$ . We have observed the clear band dispersions, which are shifted to the higher energy by 1.7 eV and show the band narrowing around 2 eV in comparison with the local density approximation calculations. In addition, the high energy multiplet structures of Cu  $3d^8$  final-states have been found around 8 - 13 eV. These results reveal that  $\text{CaCu}_3\text{Ti}_4\text{O}_{12}$  is a Mott-type insulator caused by the strong correlation effects of the Cu  $3d$  electrons well hybridized with O  $2p$  states. Unexpectedly, there exist a very small spectral weight at the Fermi level in the insulator phase, indicating the existence of isolated metallic states.

PACS numbers: 71.27.+a, 79.60.-i

---

\*Electronic address: hojun@cc.hirosaki-u.ac.jp

A-site ordered perovskite  $\text{CaCu}_3\text{Ti}_4\text{O}_{12}$  (CCTO) has generated considerable interest due to the extremely high dielectric constant ( $\epsilon$ ) as high as  $10^4$ - $10^5$  over a wide range of temperature from 100 to 600 K, which holds a promise for high performance capacitor [1]. Prior to applications, there have been many researches to identify the intrinsic mechanism of the high  $\epsilon$ . Although the consistent conclusion of the origin has not been established yet, it has been widely accepted that the high  $\epsilon$  would come from defects and/or disorder structures, e.g. a relaxor like dipole fluctuation in nanosize domain [2], an internal barrier layer capacitance [3], and the nanoscale disorder of Ca and Cu-site [4]. Generally, the origin of the high  $\epsilon$  of CCTO has been considered to be different from that of conventional ferroelectric materials, because of the absence of structural transition accompanying with the abrupt change of  $\epsilon$  around 100 K [5, 6]. In order to understand the above intrigue physical properties, it is essential that the electronic structures are clarified by direct observations. Especially, relations between the electronic structure and the strong correlation effects are central issues [7–9]. Actually, the high  $\epsilon$  and an insulator phase of CCTO can not be explained by theoretical calculations within the local density approximation (LDA), which are not considered to properly treat the strong correlation between electrons. The strong correlation effects can be also expected from the crystal structure of CCTO, which contains the  $\text{CuO}_4$  plane units in similar to the  $\text{CuO}_2$  plane of the high- $T_c$  cuprates as shown in Fig. 1 (b) [10]. Recently, it has been reported that a family compound,  $\text{CaCu}_3\text{Ru}_4\text{O}_{12}$ , shows the heavy fermion behavior and the non-Fermi liquid, supporting the importance of the strongly correlated effects [11]. Hence, it has been believed that CCTO would be a Mott-type insulator, even though the experimental band dispersions have never been observed.

Here, we first report the clear observation of band dispersions of CCTO by the angle-resolved photoemission spectroscopy (ARPES) measurements and determine the experimental electronic structure. It has revealed that the strong correlation effects of the Cu  $3d$  electrons well hybridized with O  $2p$  electrons give rise to a Mott-type insulator. Beyond, we have observed very small spectral weights at the Fermi level ( $E_F$ ) in spite of the insulator phase, indicating the existence of metallic islands which has been proposed as a possible origin of the high  $\epsilon$  [4].

High-quality CCTO single crystal was prepared by the traveling solvent floating zone method (TSFZ). ARPES experiments were performed at the beamline BL5U of UVSOR. The range of photon energies ( $h\nu$ ) is from 30 to 93 eV. The surface of samples was prepared

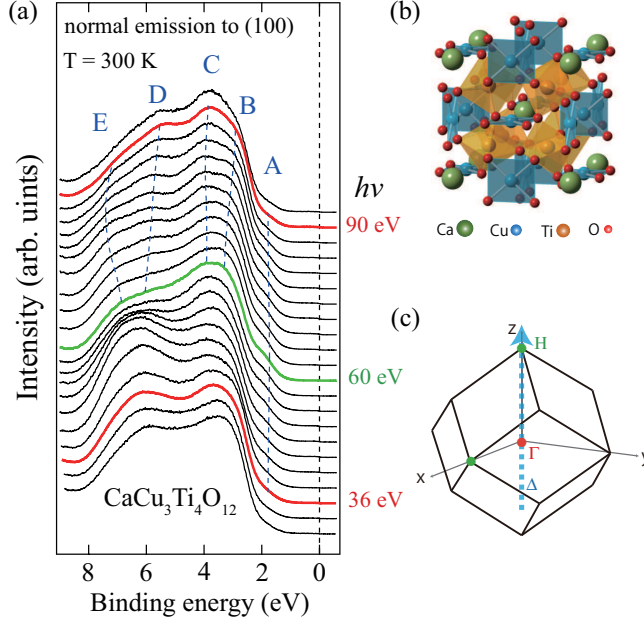


FIG. 1: (color online) (a) The EDCs along  $\Gamma H$  ( $\Delta$ ) - direction in the normal emission to the (100) plane, observed by using the photon energies from  $h\nu = 30$  to  $93$  eV at intervals of  $3$  eV. The blue dashed lines are guides for the eyes. (b) Body-centered cubic structure [10] and (c) Brillouin zone of A-site ordered perovskite  $\text{CaCu}_3\text{Ti}_4\text{O}_{12}$ .

by cleaving *in situ* in the (100) plane. Measurements were carried out at room temperature ( $T = 300$  K) in a vacuum better than  $2 \times 10^{-8}$  Pa. A wide angle acceptable MBS analyzer ( $\pm 16^\circ$ ) is used with the total energy resolution of  $165$  meV at  $h\nu = 90$  eV and the momentum resolution of  $\sim 0.02 \text{ \AA}^{-1}$ . The prepared surface of CCTO is very stable and show no sign of the progress of degradation during a typical measurement period of 12 hours. The crystal directions were determined by Laue pattern.

Measurements have been performed in the following order. First,  $h\nu$ -dependent photoemission spectroscopy (PES) measurements were performed in normal emission. This enables us to estimate the inner potential ( $V_0$ ) and determine the high symmetry points (See text for details) [12]. Next, ARPES measurements have been performed in focusing the high symmetry line in the valence regime and near  $E_F$ . The obtained experimental band dispersions were compared with the LDA calculations. Last, in order to investigate the detailed electronic structure at  $E_F$ , we have performed the low-energy angle-integrated photoemission spectroscopy (AIPES) measurements at  $h\nu = 7$  eV, which are bulk-sensitive and have the high-energy resolution of  $15$  meV, at the beamline BL7U of UVSOR.

Figure 1 (a) shows the energy distribution curves (EDCs) of CCTO in the valence-band region. The spectra have been obtained at room temperature ( $T = 300$  K) with changing  $h\nu$  from 30 to 93 eV in the normal emission to the (100) plane. With increasing  $h\nu$ , ARPES spectra trace the blue arrow along  $\Delta$ -direction in the Brillouin zone of CCTO depicted as in Fig. 1 (c). For the sake of convenience, the valence bands are divided into three regions, 0 - 2.5 eV, 2.5 - 5 eV, and 5 - 8 eV. The bands in the regions of 2.5 - 5 eV and 5 - 8 eV relatively highly disperse with intense features, while the bands in the region of 0 - 2.5 eV are not well distinguished due to weak intensity and broad band width. In the region of 0 - 2.5 eV, we observe the intensity variation of the small shoulder as a function of  $h\nu$  as designated by the letter A. The shoulder of A becomes prominent with changing  $h\nu$  from 30 to 60 eV, and then its intensity become smaller from  $h\nu = 60$  to 90 eV. This indicates that  $h\nu = 60$  eV can be a high symmetry point, even though we should be careful of the variation of the photoionization cross section ( $\sigma$ ) as  $h\nu$  changes.

In the region of 2.5 - 5 eV, there are two types of bands designated by the letters B and C. The band B disperses from 3 to 2.5 eV with the top at  $h\nu = 90$  eV and the bottom at  $h\nu = 60$  eV, while the band C shows very small dispersion around 3.8 eV reflecting the localized character. In the region of 5 - 8 eV, bands well split into two types (D and E). As  $h\nu$  closes to 90 eV, the band D has the top at 5 eV and the band E has the bottom at 7 eV. From the above results, we concluded that both  $h\nu = 60$  and 90 eV correspond to high symmetry points.  $V_0$  was estimated to be 16 eV according to the free-electron final-state model [12]. The obtained symmetry points are designated as shown in Fig. 1 (a): the EDCs at  $h\nu = 36$  eV and 90 eV correspond to  $\Gamma$ -point (red line) and that of  $h\nu = 60$  eV to H-point (green line). Beyond the above band dispersion, it is found that there is large intensity variation around 6.5 eV as  $h\nu$  closes to about 50 eV. This has been also observed in the other transition-metal oxides, where it comes from the resonance around O 2*p* edge and is not relevant to band dispersion [13]. At the same time, it means that the spectral weight of this region includes much weight of O 2*p* orbital.

Let us compare the spectral weight obtained in the angle-integrated mode of analyzer with the density of states (DOS) in the LDA calculations. Figure 2 (a) and 2 (b) show the AIPES spectrum at  $h\nu = 90$  eV and the partial DOS obtained from the LDA calculations, respectively. First, we recognize that the spectral weights near  $E_F$  do not seem to exist in this scale plot (actually, there are very small spectral weights, and we will discuss it later),

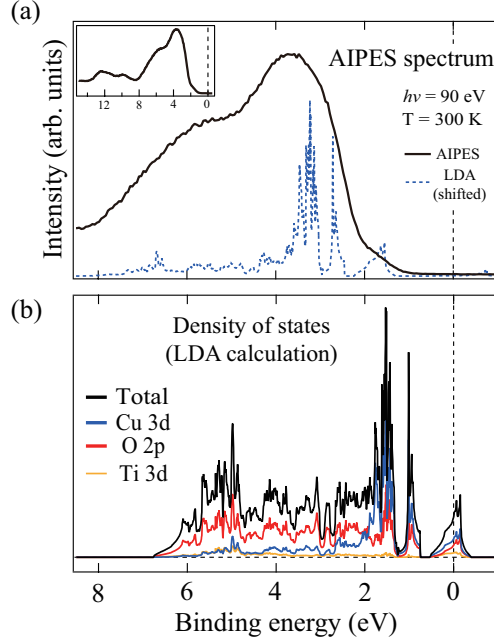


FIG. 2: (color online) (a) AIPES spectrum of CCTO obtained at  $h\nu = 90$  eV and  $T = 300$  K in valence band region. The inset shows the AIPES spectrum in wide valence band region. For comparison, the partial DOS of Cu 3d is inserted below the AIPES spectrum. (b) Total DOS and the partial DOS for the valence bands of each element, Cu 3d, O 2p, and Ti 3d in the LDA calculations.

explaining the insulator property of the electrical resistivity experiments, while the DOS of mainly Cu 3d and O 2p states exists at  $E_F$  in the LDA calculations. When we compare ARPES spectra with the DOS, the variation of the  $\sigma$  with incident photon energies should be taken into account: the  $\sigma$  of  $d$ -orbital is generally much larger than that of  $p$ -orbital by about ten times at  $h\nu = 90$  eV [14]. In Fig. 2 (a), we plot the partial DOS of Cu 3d of the LDA calculations inside AIPES spectrum, which was shifted to higher binding energy by 1.7 eV. The AIPES spectrum shows good agreement with the shifted partial DOS of Cu 3d in the LDA calculations. We find that the shoulder around 2 eV with weak intensity (band A) corresponds to the DOS at  $E_F$  in the LDA calculations. There are the intense peaks in the region from 2.5 to 8 eV which correspond to the bands B, C, D, and E in Fig. 1 (a). The bands B and C mainly consist of Cu 3d states, and the band D and E mainly come from O 2p states. On the other hand, most DOS of Ti 3d-orbital are located in the unoccupied region [Fig. 2 (b)]. In the inset of Fig. 2 (a), we have observed two peaks around 8 - 13

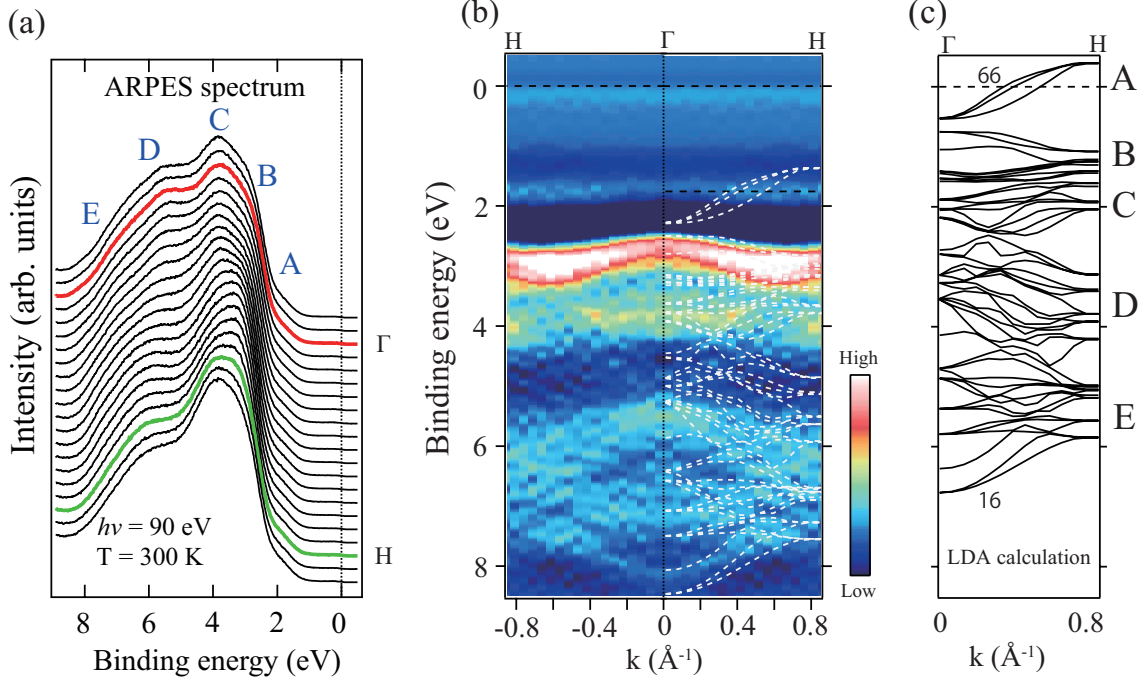


FIG. 3: (color online) (a) ARPES spectra of CCTO along  $\Delta$ -direction in the parallel to the cleaved surface (100) plane. The used photon energy is  $h\nu = 90$  eV and the measurement temperature is 300 K. (b) ARPES image obtained from the second derivatives of the EDCs. The theoretical band dispersions (white dash line), shifted by 1.7 eV, are plotted on the ARPES image. (c) Theoretical band dispersions obtained from the LDA calculations.

eV, which do not appear in the LDA calculations. The peaks are the intrinsic features of CCTO, because the two peaks have appeared in the fresh surface just after the cleaving sample and show no degradation during the measurements. In fact, it has been reported in CuO, family compound CCRO, etc. that such high energy peak structures come from Cu  $3d^8$  final-states due to multiplet effects, indicating the strong correlation effects [7, 15, 16].

Figure 3 (a) shows EDCs obtained in the angle-resolved mode of analyzer at  $h\nu = 90$  eV and  $T = 300$  K. Geometrically, the direction of the spectra is parallel to the sample surface (namely, perpendicular to the normal emission) and is also along  $\Delta$ -direction due to the symmetry of the cubic structure. Hence, both EDCs in Fig. 1 (a) and in Fig. 3 (a) represent the same band dispersions. Certainly, we recognize that the EDCs of the  $h\nu$ -dependent PES from 60 to 90 eV are very similar to the ARPES spectra, indicating that both EDCs in Fig. 1 (a) and Fig. 3 (a) are the same band dispersions. At the same time, this means that our experimental results are very reliable. Here, we can explicitly determine

the band dispersion of CCTO by comparing these two kinds of photoemission spectra with the band calculations. Figure 3 (b) is the image of the ARPES spectra obtained by the second derivatives of the EDCs. Figure 3 (c) shows the band dispersions obtained from the LDA calculations. And, the calculated band dispersions are superimposed on the ARPES image, shifting to the higher binding energy by 1.7 eV [Figure 3 (b)]. First, it should be noted that there are 51 bands in the valence band region as shown in Fig. 3 (c). Actually, the PES experiments cannot resolve these bands very closed each other due to the limitation of resolution of energy and momentum space. Therefore, the observed 5 types of band dispersions (A, B, C, D, and E) in ARPES experiments should be interpreted as a bundle of bands with the similar tendency. In the region of 0 - 2.5 eV, the EDCs show a little different behavior between ARPES and  $h\nu$ -dependent PES. The intensity variation of the band A around 2 eV in the ARPES measurements [Fig. 3 (a)] is small compared to the  $h\nu$ -dependent PES measurements [Fig. 1 (a)], which may come from the different transition probability between initial state and final state in the different methods of PES measurements. As discussed in the analysis of AIPES spectrum [Fig. 2 (a)], we can assign the band A to three bands from 64 to 66 which cross  $E_F$  and show the band dispersion of about 1 eV [Fig. 3 (c)]. Even though the exact size of band dispersion can not estimated due to the band broadening in the ARPES measurements, we find that the band width is very narrow in ARPES than in the LDA calculations [Fig. 3 (c)]. This indicates that the band A is more localized than the expectation of the LDA calculations. In the region of 2.5 - 5 eV, the dispersion of band C with the most intense peak has been more clearly observed than in the  $h\nu$ -dependent PES measurements. The band C disperses from 3.8 eV at  $\Gamma$ -point (red line) to 3.5 eV at H - point (green line) showing small upturn behavior [Fig. 3 (a)]. This behavior could not be well resolved in  $h\nu$ -dependent ARPES due to the rough step of  $h\nu$  ( $\Delta h\nu = 3 \text{ eV} \sim k = 0.08 \text{ \AA}^{-1}$  around  $h\nu = 90 \text{ eV}$ ). It is also observed that there is a shoulder around 2.7 eV indicating existence of bands. This band corresponds to the band B and is more clearly observed in  $h\nu$ -dependent PES than in ARPES. The band B and C are assigned to bands from 60 to 63 and bands from 55 to 59, respectively. In the region of 5 - 8 eV, ARPES data also show the well splitted bands, D and E. These bands consist of many bands from 16 to 50. As shown above, the tendency of band dispersions of ARPES experiments is well consistent with those of the LDA calculations, except for the shift to the higher binding energy by about 1.7 eV, the band narrowing around 2 eV, and the high-energy multiplet

structures of Cu  $3d^8$  final-states around 8 -13 eV.

Here, we assign the difference of the electric structure between ARPES experiments and LDA calculation to strong correlation effects as follows. According to Mott-Hubbard model, the strong correlation effects separate the DOS into the upper Hubbard band in unoccupied region and the lower Hubbard band in occupied region as in many perovskite systems [7]. In the case of CCTO, the hybridized bands of Cu  $3d$  and O  $2p$  states were shifted to the higher binding energy by about 1.7 eV in comparison with the LDA calculations, showing a little different behavior compared to the simple Mott-Hubbard model. However, this is not surprising because the Cu  $3d$  states have about 9 electrons in the occupied region and about 1 electron in the unoccupied region and are well hybridized with O  $2p$  states in spite of the strong correlation effects. In fact, the similar band structures can be found in earlier studies of CuO and the high- $T_c$  cuprates [7, 15]. For the reason of such a behavior, we speculate that the hybridized bands in the  $\text{CuO}_4$  unit are localized as a cluster due to the separation between the  $\text{CuO}_4$  units as shown in the crystal structure of Fig. 1 (b). To evaluate the explicit size of the repulsive Coulomb interaction energy, we are now proceeding inverse photoemission spectroscopy studies which provide the electronic structure in the unoccupied region. The second one is the narrowing of band width around 2 eV. When the electrons are localized due to large repulsive Coulomb interactions, and the dispersion become small and the band width should be narrow, consequently, as observed in strongly correlated  $f$ -electrons systems [17]. The third one is the high energy multiplet structures of Cu  $3d^8$  final-states around 8 - 13 eV, indicating atomic-like behaviors caused by strong correlation effects as in CuO and CCRO [7, 15, 16, 18].

Finally, let us discuss the small spectral weights at  $E_F$ . Figure 4 (a) is the enlarged plot of EDCs at  $\Gamma$  and H - points in Fig. 3 (a). We find that there is a very small spectral weight at  $E_F$  in spite of the insulator phase in the electrical resistivity measurements. A possibility, Ti  $3d$  states remains at  $E_F$ , should be ruled out because CCTO would show the metallic properties if Ti  $3d$  states exist at  $E_F$ . The another possibility is the metallic phase caused by the surface state of CCTO, because the PES spectra, obtained by using  $h\nu = 20 - 100$  eV, are surface sensitive as explained by the universal curve [19]. It is well known that the mean free path in solids becomes sufficiently long to probe the bulk properties by using around 7 eV photons [20]. Therefore, we have performed the AIPES measurements at  $h\nu = 7$  eV as shown in Fig. 4 (b). The spectral weight at  $E_F$  (open circle) has been



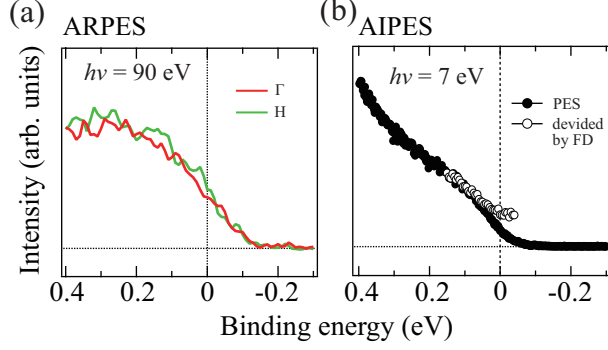


FIG. 4: (color online) (a) The enlarged ARPES spectra at  $\Gamma$  and H - points near  $E_F$  in Fig. 3 (a). (b) The bulk sensitive AIPES spectra near  $E_F$  at  $h\nu = 7$  eV. The solid circle is the AIPES spectrum and the open circle is the spectral weight near  $E_F$  obtained by dividing the AIPES spectrum by the Fermi Dirac function, which is convoluted by the energy resolution of 15 meV and the measurement temperature of 300 K.

recovered by dividing the AIPES spectra (solid circle) by the Fermi Dirac function, which is convoluted by the energy resolution and the measurement temperature [17, 21]. There exist the unambiguous spectral weights at  $E_F$ . In fact, Zhu et al. have suggested that there are nano-size metallic islands due to the interchange between A-site elements, Ca and Cu, causing the extremely large  $\epsilon$  [4].

In summary, we first present the experimental band structures of CCTO by using the ARPES and  $h\nu$ -dependent PES measurements. In comparison with the LDA calculations, it has been revealed that the band structures are located in the higher binding energy by 1.7 eV and the Cu 3d - O 2p hybridization bands around 2 eV are narrow. And, the multiplet structures of Cu 3d<sup>8</sup> final-states are observed around the binding energies of 8 - 13 eV. Such ARPES results have revealed the strong correlation effects of CCTO. Beyond the above results, we have also observed the very small spectral weight at  $E_F$  in the insulator phase, implying the existence of metallic islands.

## Acknowledgments

The authors are grateful to S. Nakajima for technical assistance.

---

- [1] M. A. Subramanian, D. Li, N. Duan, B. A. Reisner, and A. W. Sleight, *J. Solid State Chem.* **151**, 323 (2000).
- [2] C. C. Homes, T. Vogt, S. M. Shapiro, S. Wakimoto, and A. P. Ramirez, *Science* **293**, 673 (2001).
- [3] S. Y. Chung, I. D. Kim, and S. J. L. Kang, *Nat. Mater.* **3**, 774 (2004).
- [4] Y. Zhu, J. C. Zheng, L. Wu, A. I. Frenkel, J. Hanson, P. Northrup, and W. Ku, *Phys. Rev. Lett.* **99**, 037602 (2007).
- [5] A. P. Ramirez, M. A. Subramanian, M. Gardel, G. Blumberg, D. Li, T. Vogt, and S. M. Shapiro, *Solid State Commun.* **115**, 217 (2000).
- [6] A. P. Litvinchuk, C. L. Chen, N. Kolev, V. N. Popov, V. G. Hadjiev, M. N. Iliev, R. P. Bontchev, and A. J. Jacobson, *phys. stat. sol. (a)* **195**, 453 (2003).
- [7] M. Imada, A. Fujimori, and Y. Tokura, *Rev. Mod. Phys.* **70**, 1039 (1998).
- [8] G. Kotliar, S. Y. Savrasov, K. Haule, V. S. Oudovenko, O. Parcollet, and C. A. Marianetti, *Rev. Mod. Phys.* **78**, 865 (2006).
- [9] L. He, J. B. Neaton, Morrel, H. Cohen, D. Vanderbilt, and C. C. Homes, *Phys. Rev. B* **65**, 214112 (2002).
- [10] Y. W. Long, N. Hayashi, T. Saito, M. Azuma, S. Muranaka, and Y. Shimakawa, *Nature* **458**, 60 (2009).
- [11] W. Kobayashi, I. Terasaki, J. ichi Takeya, I. Tsukada, and Y. Ando, *J. Phys. Soc. Jpn.* **73**, 2373 (2004).
- [12] Hufner, *Photoelectron Spectroscopy* (Springer, 1995).
- [13] K. Breuer, D. M. Goldberg, K. E. Smith, M. Greenblatt, and W. McCaroll, *Solid State Commun.* **94**, 601 (1995).
- [14] J. J. Yeh and I. Lindau, *Atom Data Nucl. Data* **32**, 1 (1985).
- [15] J. Ghijsen, L. H. Tjeng, J. van Elp, H. Eskes, J. Westerink, G. A. Sawatzky, and M. T. Czyzyk, *Phys. Rev. B* **38**, 11322 (1988).

- [16] N. Hollmann, Z. Hu, A. Maignan, A. Gunther, L.-Y. Jang, A. Tanaka, H.-J. Lin, C. T. Chen, P. Thalmeier, and L. H. Tjeng, arXiv:1211.2984v1 (2012).
- [17] H. J. Im, T. Ito, H. D. Kim, S. Kimura, K. E. Lee, J. B. Hong, Y. S. Kwon, A. Yasui, and H. Yamagami, Phys. Rev. Lett. **100**, 176402 (2008).
- [18] H. Eskes, L. H. Tjeng, and G. A. Sawatzky, Phys. Rev. B **41**, 288 (1990).
- [19] M. P. Seah and W. A. Dench, Surf. Interface Anal. **1**, 2 (1979).
- [20] T. Kiss, F. Kanetaka, T. Yokoya, T. Shimojima, K. Kanai, S. Shin, Y. Onuki, T. Togashi, C. Zhang, C. T. Chen, et al., Phys. Rev. Lett. **94**, 057001 (2005).
- [21] T. Greber, T. J. Kreutz, and J. Osterwalder, Phys. Rev. Lett. **79**, 4465 (1997).